



HAL
open science

Pulsed flow turbine design recommendations

Florian Hermet, Nicolas Binder, Jérémie Gressier

► **To cite this version:**

Florian Hermet, Nicolas Binder, Jérémie Gressier. Pulsed flow turbine design recommendations. 14th European Conference on Turbomachinery Fluid dynamics & Thermodynamics (ETC14), Apr 2021, Gdansk, Poland. pp.0. hal-03209283

HAL Id: hal-03209283

<https://hal.science/hal-03209283>

Submitted on 27 Apr 2021

HAL is a multi-disciplinary open access archive for the deposit and dissemination of scientific research documents, whether they are published or not. The documents may come from teaching and research institutions in France or abroad, or from public or private research centers.

L'archive ouverte pluridisciplinaire **HAL**, est destinée au dépôt et à la diffusion de documents scientifiques de niveau recherche, publiés ou non, émanant des établissements d'enseignement et de recherche français ou étrangers, des laboratoires publics ou privés.



Open Archive Toulouse Archive Ouverte (OATAO)

OATAO is an open access repository that collects the work of some Toulouse researchers and makes it freely available over the web where possible.

This is a publisher's version published in: <https://oatao.univ-toulouse.fr/27767>

Official URL:

To cite this version :

Hermet, Florian and Binder, Nicolas and Gressier, Jérémie Pulsed flow turbine design recommendations. (2021) In: 14th European Conference on Turbomachinery Fluid dynamics & Thermodynamics (ETC14), 12 April 2021 - 16 April 2021 (Gdansk, Poland).

Any correspondence concerning this service should be sent to the repository administrator:

tech-oatao@listes-diff.inp-toulouse.fr

PULSED FLOW TURBINE DESIGN RECOMMENDATIONS

F. Hermet - N. Binder - J. Gressier

ISAE-SUPAERO, Université de Toulouse, France
florian.hermet@isae-supaero.fr

ABSTRACT

A preliminary analysis of turbine design, fit for pulsed flow is proposed in this paper. It focuses on an academic 2D configuration using inviscid flows, since pressure loads due to wave propagation are several order of magnitude higher than friction and viscous effects do not significantly impinge on the inviscid part. As such, a large parametric study is carried out using the design of experiments methodology. A performance indicator adapted to unsteady environment is carefully defined before detailing the factors chosen for the design of experiments. Since the number of factors is substantial, a screening design to identify the factors influence on the output is first established. The non-influential factors were then omitted in a more quantitative study of the output law. The surface response calculation allows to determine the factors level favouring the best output. Consequently, the main trends in the turbine design driven by a pulsed flow can be stated.

KEYWORDS

pulsed flow, turbine design, design of experiment

NOMENCLATURE

α_{out}	Blade metal angle	L	Distance
Δt_{cycle}	Cycle time	$P_{s,outlet}$	Static outlet pressure
Δt_{open}	Opening phase time	$P_{t,open}$	Total pressure during the opening phase
\dot{m}	Mass flow rate	r	Gaz constant
s	Entropy	\dot{W}	Work turbine
T_t	Total temperature	σ	Standard deviation
x_c	Axial chord	h_{rotor}	Rotor pitch
h_{stator}	Stator pitch	h_t	Total enthalpy
<i>Subscripts</i>			
in	inlet	out	outlet

INTRODUCTION

In many applications, the turbine is subject to temporal variations of its inlet conditions. The most extreme case is found when the turbine is involved in a thermodynamic cycle including isochoric combustion process. During the last decade, the uprising interest in aeronautics for isochoric combustion cycles has stimulated research on axial turbines supplied by severe unsteadiness. However, major contributions to this question are credited to the automotive turbocharger community. In Baines (2010), there is a detailed summary of nearly 20 years of research on pulsed flow in radial turbines. This review highlights the progress and contradictions in the scientific community, particularly regarding the pulsed flow influence on turbine performance. The complexity of this problem comes from the coupling between different phenomenon involving time scales which are not easily separate (pulse time scale, propagative time

scale, advective time scale, ...). Moreover, the definition of a turbine performance indicator is made complex by this severe flow unsteadiness. This partly explains why there is no consensus on the pulsed flow influence in turbines, and more specifically whether or not the performance could take some benefits of the unsteadiness. Anyway, a necessity to adapt the design process to the unsteady environment is rising in the literature (Liu & Copeland 2020)

The complexity of the geometries involved in the different studies of the literature is also an additional difficulty to enlighten comprehension. Recent numerical work, Hermet et al. (2019), focuses on that question through a simplified cascade approach. It has been shown that instantaneous loading differs from the quasi-steady approach in response to a rapid increase in turbine inlet pressure. The relevant time scale of the inlet perturbation associated with the additional work extracted by the turbine were also identified by the authors. In short, it appears that the curvature intensifies the different pressure effects during the wave propagation. Thus, a compression wave propagating in the direction of the flow overloads the blades, compared with a quasi-steady transformation. Other combinations of wave nature (compression or expansion) and direction (upstream or downstream) have different consequences. For example a stream-wise expansion under-loads the blades. In pulsating flows, a succession of waves of different nature and direction of propagation happens. The net benefit of unsteady effects over a complete cycle thus needs to be quantified. It is the main objective of this paper, together with a clear statement of which geometrical parameter is likely to promote the unsteady performance.

The present work is thus in a direct continuation of the work of Hermet et al. (2019). The physics of pulsed flow is terribly complex. Therefore, the analysis is conducted thanks to parametric studies for which numerical design of experiment (DOE) are built. The adequate performance indicator is firstly discussed before describing the selected factors. Because of the large number of factors involved, an initial screening phase has been conducted. This allows to identify the influence of each factor on the response. Non-influential factors are then discarded for a more quantitative study of the output law. The quantitative prediction is built by calculating the response surface. As a conclusion the main trends observed in 2D are exploited to propose first recommendations for the design of turbines able to take some benefits from the large unsteadiness of a pulsating flow.

METHODOLOGY

The parametric study focuses on the simulation of stabilized pulsed flow through simplified cascade approaches of the stator and rotor thanks to in-house IC³ solver, forked from CharLES^X solver, Brès et al. (2017). IC³ is based on the resolution of the compressible formulation of Navier-Stokes equations in their conservative form, spatially filtered, on an unstructured mesh using a finite volume method. An explicit third-order Runge-Kutta scheme is used for time advancement while an essentially non-oscillatory (ENO) second-order shock-capturing scheme is applied to compute flux. A stabilized pulsed flow is a perfectly periodic flow, similar to flows caused by the cyclic opening and closing of a valve separating the combustion chamber from the turbine. The choice of the performance criteria selected for the response of the DOE is first discussed. The selected factors of the design of experiments are then presented.

Response of design of experiments

Most of performance indicators used in the turbocharger literature do not take into account the full complexity of flow unsteadiness, as shown in Lee et al. (2017). In order to design a turbine under pulsed flow, the performance indicators of the turbine must be clearly defined.

For this, it is appropriate to remind the mass conservation equation as well as the first and second thermodynamics principles of an adiabatic unsteady system ($\dot{Q} = 0$), eq. (1).

$$\left\{ \begin{array}{l} \dot{m}_{in}(t) - \dot{m}_{out}(t) = \frac{d}{dt} \int_V \rho(t) dV \\ \dot{m}_{in}(t)h_{t,in}(t) - \dot{m}_{out}(t)h_{t,out}(t) = \frac{d}{dt} \int_V \rho(t)e_t(t)dV + \dot{W} \\ \dot{m}_{in}(t)s_{in}(t) - \dot{m}_{out}(t)s_{out}(t) + \int_V \dot{S}_{gen}'''(t)dV = \frac{d}{dt} \int_V \rho(t)s(t)dV \end{array} \right. \quad (1)$$

For stabilized pulsed flow (perfectly periodic), the eq. (1) can be simplified by integrating them over the inlet valve cycle duration. Indeed, the temporal variations of the storage effects are canceled out over the cycle. The system of eq. (1) then reduces to the eq. (2).

$$\left\{ \begin{array}{l} \int_{\Delta t_{cycle}} \dot{m}_{in} dt - \int_{\Delta t_{cycle}} \dot{m}_{out} dt = 0 \\ \int_{\Delta t_{cycle}} \dot{m}_{in} h_{t,in} dt - \int_{\Delta t_{cycle}} \dot{m}_{out} h_{t,out} dt = \int_{\Delta t_{cycle}} \dot{W} dt \\ \int_{\Delta t_{cycle}} \dot{m}_{in} s_{in} dt - \int_{\Delta t_{cycle}} \dot{m}_{out} s_{out} dt + \int_{\Delta t_{cycle}} \int_V \dot{S}_{gen}''' dV dt = 0 \end{array} \right. \quad (2)$$

From the eq. (2), turbine performance indicators over a valve cycle can be defined. The aim of the paper is to give design trends that will extract the maximum energy from the flow. It is then necessary to compare the energy extracted during a cycle to the energy injected into the turbine in a cycle, see the eq. (3). When $\eta_{cycle} = 1$, the turbine extracts all the energy from the flow. This efficiency can be negative when flow waves cause a reversal in the direction of the aerodynamic force applied to the blades. In this case the system operates as a compressor.

$$\eta_{cycle} = \frac{\int_{\Delta t_{cycle}} \dot{W}(t) dt}{\int_{\Delta t_{cycle}} \dot{m}_{in}(t) c_p T_{t,in}(t) dt} \quad (3)$$

The indicator (3) is not an efficiency as usually found in the literature, and should not be considered as such. It corresponds to the output for the various factorial combinations considered in this paper, allowing a fair comparison between different pulsating profiles. It could be interpreted as a recovery coefficient. Now the factors that may influence this output are described.

Factors of design of experiments

The system design is not only based on the turbine geometry, but also on the inlet and outlet boundary conditions. Indeed, the geometry allows to extract energy from the flow while the inlet and outlet boundary conditions¹ contributes to create favorable flow conditions for the work extraction.

¹It is also the case of the geometry since it modifies the flow physics.

Geometric parameters

Several assumptions have been made to reduce the number of geometric factors. First of all, the stator and rotor cascades were taken thin and two-dimensional. Cascades are built with the eq. (4). Angles at the leading edge of cascades in relation to the direction of the inlet flow was taken to be zero. Moreover, the axial length of the stator and the rotor blades are considered identical.

$$y(x) = -\frac{4 \tan(\alpha_{out})}{\pi^2} \left[1 + \sin\left(\frac{\pi}{2} \sin\left(\frac{\pi}{2} \frac{x}{x_c}\right)\right) \right] \quad (4)$$

In addition to the blades geometrical parameters, the lengths between boundary conditions and the blades are significant for pulsed flows. They influence the location of the waves interaction in the domain. The length between the rotor trailing edge and the outlet boundary condition was considered very large to eliminate this parameter. The DOE geometric factors are shown in figure (1).

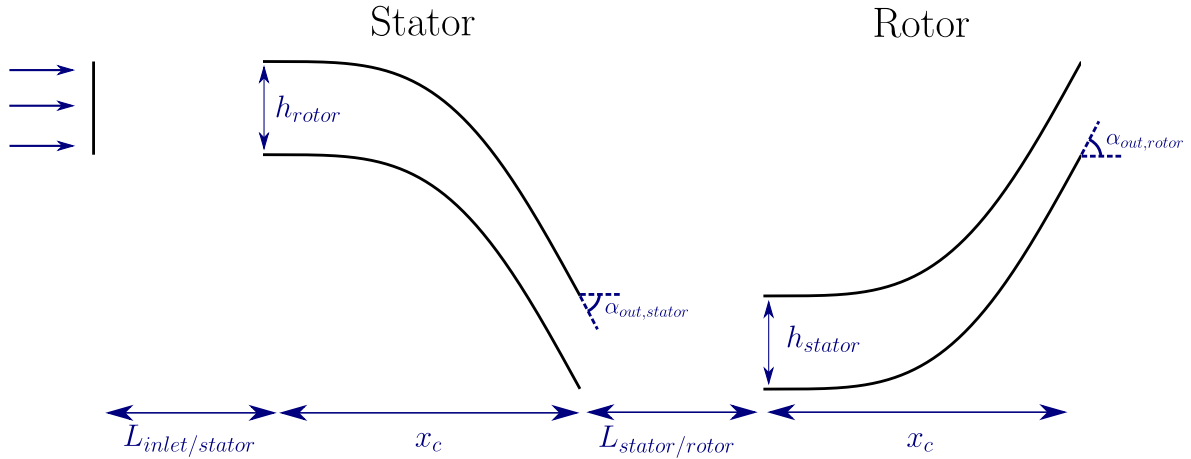


Figure 1: Geometry parameters

Dynamic parameters

The inlet valve cycle was chosen as a square-wave. The opening and closing of the valve is instantaneous. During the opening phase, total pressure and total temperature are prescribed. A wall boundary condition is imposed during the closing phase. Under these assumptions, it takes 4 factors to set up the valve cycle : $P_{t,open}$, $T_{t,open}$, Δt_{cycle} and Δt_{open} . To set up the simulation, an outlet pressure condition is applied : $P_{s,outlet}$. The calculation information at the interface between the stator and rotor cascade is exchanged via a sliding mesh model, rotor speed must be given : U_{rotor} . The rotor speed is considered constant in numerical simulations. Indeed, the assumption is made that the valve cycles are much too fast for the rotor to adapt to the flow changes. All the other boundary conditions are supposed periodic.

Fluid parameters

The analyzed fluid is air. Thanks to the ideal gas law, the flow density is known. Only inviscid simulations are performed in this paper. Indeed, comparisons of large eddy simulations with inviscid simulations of transient flow within a 2D turbine cascade, carried out at the depart-

ment and currently being published, show that viscosity has no influence on the work prediction during the transient regime. No fluid parameter is added in the DOE factors.

Dimensionless factors

The system behavior law involves $n = 13$ dimensional parameters and $k = 3$ fundamental units. Thanks to Vaschy-Buckingham's theorem, the behavior law can be determined with $n - k = 10$ dimensionless parameters. The dimensionless factors of the design of experiments are listed in the table (1). The most of the dimensionless factors are relatively easy to understand since they are usually used in steady state flow turbine. However, some parameters, specific to pulsed flow, need to be specified. Π_{10} represents the cycle ratio while Π_5 and Π_6 set, partly, the interaction wave locations. Π_9 give an indication on the distance travelled by a wave during Δt_{cycle} . Indeed, $\sqrt{rT_{t,open}}$ is similar to sound speed, thus, $\Pi_9 = 1$ means that a wave propagating at the sound speed has traveled x_c during Δt_{cycle} .

The factor range of variation is also presented in the table (1). These ranges are large since the regions of the experiment domain that lead to the best performance were unknown at the beginning of the study. The ranges are centered and reduced between -1 and $+1$.

	Π_1 h_{stator}/x_c	Π_2 h_{rotor}/x_c	Π_3 $\alpha_{out,stator}$	Π_4 $\alpha_{out,rotor}$	Π_5 $L_{inlet/stator}/x_c$
Real	[0.1 ; 0.8]	[0.1 ; 0.8]	[40° ; 80°]	[40° ; 80°]	[0.1 ; 2.0]
Coded	[-1 ; +1]	[-1 ; +1]	[-1 ; +1]	[-1 ; +1]	[-1 ; +1]
	Π_6 $L_{stator/rotor}/x_c$	Π_7 $P_{t,open}/P_{s,outlet}$	Π_8^2 U_{rotor}/V_θ	Π_9 $\Delta t_{cycle} \sqrt{rT_{t,open}}/x_c$	Π_{10} $\Delta t_{open}/\Delta t_{cycle}$
Real	[0.1 ; 1.0]	[1.2 ; 3.0]	[0.25 ; 0.75]	[0.5 ; 5.0]	[0.1 ; 0.9]
Coded	[-1 ; +1]	[-1 ; +1]	[-1 ; +1]	[-1 ; +1]	[-1 ; +1]

Table 1: Factors and experimental domain of screening design.

MOST INFLUENTIAL FACTORS

The design of experiments is built with the JMP[©] (1989-2019) software. To determine the factors influence on output, a two-stage screening design was selected. In this screening design, the level of each factor corresponds to the boundaries of the variation range, i.e. $+1$ and -1 as a coded variable. Consequently, the predicted output law is linear. The experimental design selected is a *fractional factorial* design, see Goupy (2001) for more information. The simulations number of fractional design is equal, here, to $2^{n-p} = 2^{10-6} = 16$. Screening design is listed in the table (2).

² $V_\theta = f(\Pi_7, \Pi_3, \sqrt{rT_{t,open}})$, corresponds to the tangential velocity at the trailing edge of stator during the opening phase, assuming that all the expansion takes place in this stage.

N°	Π_1	Π_2	Π_3	Π_4	Π_5	Π_6	Π_7	Π_8	Π_9	Π_{10}	η [%]	$\frac{\sigma_{\dot{W}(t)}}{\langle \dot{W}(t) \rangle}$	Compressor [%]
1	-1	+1	-1	-1	+1	-1	+1	-1	+1	-1	2.9	4.0	50.0
2	+1	+1	+1	+1	+1	+1	+1	-1	-1	-1	10.9	0.3	0.0
3	+1	-1	-1	-1	-1	+1	+1	+1	+1	-1	-0.02	2.7	70.0
4	-1	+1	-1	+1	-1	+1	-1	+1	-1	+1	2.8	0.5	3.0
5	+1	+1	+1	-1	-1	-1	-1	+1	+1	+1	3.0	0.3	0.0
6	-1	-1	+1	+1	-1	-1	+1	+1	-1	-1	2.1	1.5	25.0
7	+1	+1	+1	+1	+1	+1	+1	+1	+1	-1	19.0	1.5	28.0
8	+1	+1	+1	+1	+1	+1	+1	+1	-1	+1	22.0	0.2	0.0
9	+1	+1	+1	+1	+1	+1	+1	-1	+1	+1	13.0	0.1	0.0
10	+1	+1	+1	+1	+1	+1	-1	+1	+1	+1	2.8	0.3	0.0
11	+1	+1	+1	+1	+1	-1	+1	+1	+1	+1	24.1	0.1	0.0
12	+1	+1	+1	+1	-1	+1	+1	+1	+1	+1	24.2	0.1	0.0
13	+1	+1	+1	-1	+1	+1	+1	+1	+1	+1	24.0	0.3	0.0
14	+1	+1	-1	+1	+1	+1	+1	+1	+1	+1	14.3	0.5	0.0
15	+1	-1	+1	+1	+1	+1	+1	+1	+1	+1	3.0	0.2	0.0
16	-1	+1	+1	+1	+1	+1	+1	+1	+1	+1	24.2	0.5	0.0

Table 2: Screening design and results associated.

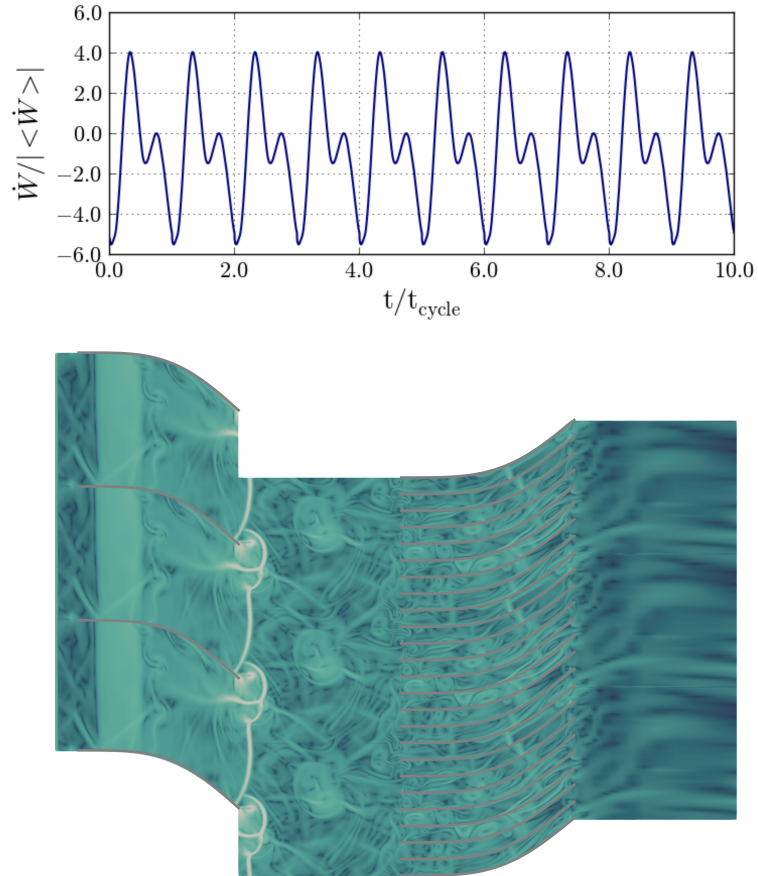


Figure 2: Above: Temporal evolution of $\dot{W}(t)$. $\dot{W} < 0$ corresponds to compressor mode. Below: Instantaneous visualization of the density gradient. Simulation $n^\circ 3$.

Screening design results

Screening design results are shown in the table (2). Two additional responses beside the recovery efficiency η are proposed. Since the rotational speed is fixed, the brutal decrease of mass-flow can make the compressor operating mode appear. The relative proportion of time in which this happens is quoted in %. Also, the standard deviation of the work signal is reported in order to quantify the loading fluctuations. The recovery efficiency of many simulations is close to $\eta_{cycle} = 0$, the turbine extracts almost no energy from the flow over a cycle. The system alternates between turbine and compressor phases. The balance between these modes is particularly visible on the temporal evolution of the $\dot{W}(t)$ for the simulation $n^{\circ}3$ in figure (2). Compressor modes are driven by waves that generate a greater force on suction side of the blade than on pressure side. The temporal evolution of $\dot{W}(t)$ shows behaviors in adequacy with the results of Hermet et al. (2019). The valve opening causes a shock wave propagation which generates a work increase. The valve closing generates an expansion wave which causes a work decrease. An instantaneous visualization of the density gradient is also shown in figure (2). This instantaneous visualization highlights the flow complexity.

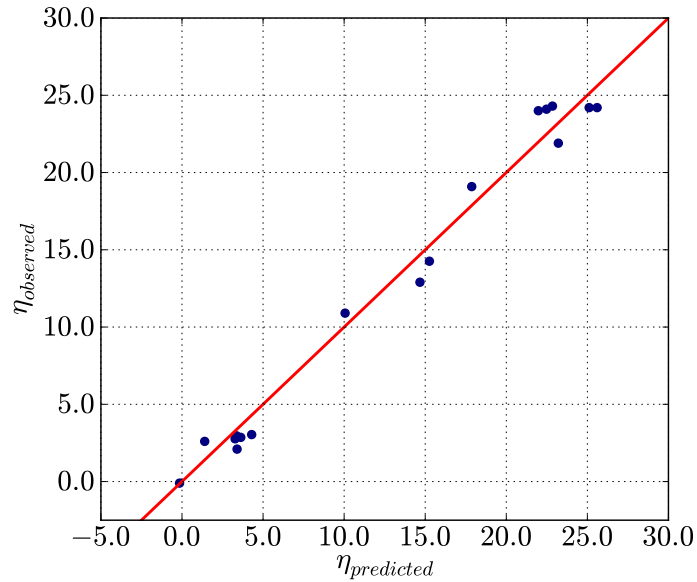


Figure 3: Prediction of screening design. $R^2 = 0.98$.

The linear prediction extracted from the screening phase is given in the figure (3). It shows a fair accuracy ($R^2 = 0.98$). Moreover, the distribution of the measured values in the observed performance range is relatively homogeneous, which gives confidence in the behavioral law prediction, and legitimate the conclusions regarding the true influence of the different factors.

For numerical experimental designs, the natural variability of the output can be considered as negligible. As a result, all factors in the design of experiments are statistically significant on system output. However, some factors may be neglected by comparing the sensitivity values of the prediction model. A factor was considered to be non-influential on the response when its sensitivity was less than 5% of the maximum sensitivity of the model.

Π_1 h_{stator}/x_c	Π_2 h_{rotor}/x_c	Π_3 $\alpha_{out,stator}$	Π_4 $\alpha_{out,rotor}$	Π_5 $L_{inlet,stator}/x_c$
✓	✓	✓	✗	✗
Π_6 $L_{stator,rotor}/x_c$	Π_7 $P_{t,open}/P_{s,outlet}$	Π_8 U_{rotor}/V_θ	Π_9 $\Delta t_{cycle}\sqrt{rT_{t,open}}/x_c$	Π_{10} $\Delta t_{open}/\Delta t_{cycle}$
✗	✓	✓	✗	✓

Table 3: Factors influence on output. ✓ is associated with an influential factor while ✗ is related to a non-influential factor.

The sensitivity analysis shows that only 6 factors have a significant role in stage performance. The influence of these factors is further investigated by calculating the response surface. Understanding in details why factors ($\alpha_{out,rotor}$, $L_{inlet,stator}/x_c$, $L_{stator,rotor}/x_c$ and $\Delta t_{cycle}\sqrt{rT_{t,open}}$) do not influence the turbine recovery efficiency is difficult with such a flow complexity. However the spatial distribution of the time averaged energy recovered show no sensitivity to these parameters. This result will not be presented here.

SURFACE RESPONSE

The reduction of the number of factors makes it possible to carry out a more quantitative study of the system output thanks to response surface methodology, Goupy (2001). The response surface modeling allows to determine the factor which optimize the output. For this design of experiment, the behavior law prediction is done by a quadratic function, see eq. (5) with x_i each selected factors.

$$y = \bar{y} + \sum_i (\lambda_i x_i + \gamma_i x_i^2) + \sum_i \sum_{j, j \neq i} \beta_{i,j} x_i x_j \quad (5)$$

In order to achieve a quadratic prediction of the output law, 3 levels for each factor must be considered in the simulations. In addition to the high +1 and low levels -1, the central level 0 is added. For the calculation, the stator and rotor channels must be multiple of each other. The central value is then adjusted for h_{stator}/x_c and h_{rotor}/x_c . The level of factors is indicated in the table (4). In the same way as the screening design, the experimental design is constructed using JMP[®] (1989-2019). In order to minimize the simulations number, a D-optimality criterion has been adopted for the design of experiment, see Goupy (2001). The surface response design is based on 28 simulations for 6 factors. The levels of the non-influential factors on the output, namely : $\Pi_4 = \alpha_{out}$, $\Pi_5 = L_{inlet,stator}/x_c$, $\Pi_6 = L_{stator,rotor}/x_c$, and $\Pi_9 = \Delta t_{cycle}rT_{t,open}/x_c$, were taken at their high level +1 to carry out simulations.

	Π_1 h_{stator}/x_c	Π_2 h_{rotor}/x_c	Π_3 $\alpha_{out,stator}$
Coded	[-1, -0.14, +1]	[-1, 0.14, +1]	[-1, 0, +1]
Real	[0.1, 0.4, 0.8]	[0.1, 0.4, 0.8]	[40°, 60°, 80°]
	Π_7 $P_{t,open}/P_{s,outlet}$	Π_8 U_{rotor}/V_θ	Π_{10} $\Delta t_{open}/\Delta t_{cycle}$
Coded	[-1, 0, +1]	[-1, 0, +1]	[-1, 0, +1]
Real	[1.2, 2.1, 3.0]	[0.25, 0.5, 0.75]	[0.1, 0.5, 0.9]

Table 4: Factors and experimental domain of surface response design.

Surface response design results

The results of the experimental design are provided in table (5). The response surface accuracy can be examined by investigating figure (4). It shows that the output law is very well modeled by the response surface ($R^2 = 0.99$). The spatial distribution of the measured values in the observed performance range is relatively homogeneous, which ensures that the predicted output law can be trusted. The model quality is also assessed on the residual value $\epsilon_i = y_i - \hat{y}_i$, figure (4). The residuals are small and have no outliers.

N°	Π_1	Π_2	Π_3	Π_7	Π_8	Π_{10}	η [%]	$\frac{\sigma_{\dot{W}(t)}}{\langle \dot{W}(t) \rangle}$	Compressor [%]
1	-1	-1	-1	-1	+1	0	-0.03	1.6	66.0
2	-1	-1	-1	+1	-1	-1	-1.04	3.1	50.0
3	-1	-1	0	-1	-1	+1	-0.42	0.3	100
4	-1	-1	+1	-1	0	-1	-0.08	4.9	58.0
5	-1	-1	+1	+1	+1	+1	-0.32	0.2	100
6	-1	+1	-1	-1	-1	-1	1.46	14.0	48.0
7	-1	+1	-1	+1	+1	+1	5.2	0.6	3.4
8	-1	+1	+1	-1	+1	+1	1.96	0.1	0.0
9	-1	+1	+1	+1	-1	+1	6.47	0.1	0.0
10	-0.14	-0.14	-1	0	0	+1	0.01	13.3	49
11	-0.14	-0.14	0	0	+1	-1	0.3	21.0	49.8
12	-0.14	-0.14	0	+1	0	0	0.01	13.0	50.0
13	-0.14	-0.14	+1	0	-1	0	-0.03	25	50.0
14	-1	+1	0	0	0	0	16.5	0.8	1.8
15	+1	-1	0	-1	-1	-1	-0.01	29.0	41.0
16	+1	-1	-1	+1	+1	+1	-0.53	0.4	97
17	+1	-1	+1	-1	+1	+1	-1.75	0.4	100
18	+1	-1	+1	+1	-1	+1	-3.9	0.1	100
19	+1	-1	0	0	0	0	0.01	50.0	50.0
20	+1	+1	-1	-1	+1	+1	11.9	0.5	3.4
21	+1	+1	-1	+1	-1	+1	23.2	0.3	1.8
22	+1	+1	-1	+1	+1	-1	3.4	13.5	55.0
23	+1	+1	+1	-1	-1	+1	16.2	0.2	0.0
24	+1	+1	+1	-1	+1	-1	2.9	23.0	52.0
25	+1	+1	+1	+1	-1	-1	29.4	1.3	13.5
26	+1	+1	+1	+1	+1	-1	19.1	2.3	35.0
27	+1	+1	+1	+1	+1	+1	24.3	0.2	0.0
28	+1	-1	+1	+1	+1	+1	3.0	0.3	0.0
29	+1	+1	-1	+1	+1	+1	14.3	0.3	0.0
30	+1	+1	+1	-1	+1	+1	9.0	0.3	0.0

Table 5: Surface response design selected and results associated.

It is interesting to focus on a few particular simulations showing original behaviors. Simulations $n^\circ 17$ or $n^\circ 18$ reveal that it is possible, with the wrong set of parameters, to design a system operating exclusively in compressor mode, whereas the target is to design a turbine. The $n^\circ 25$ shows a fairly marked compressor mode over a cycle (13.5%) whereas this simulation leads to the highest recovery efficiency observed.

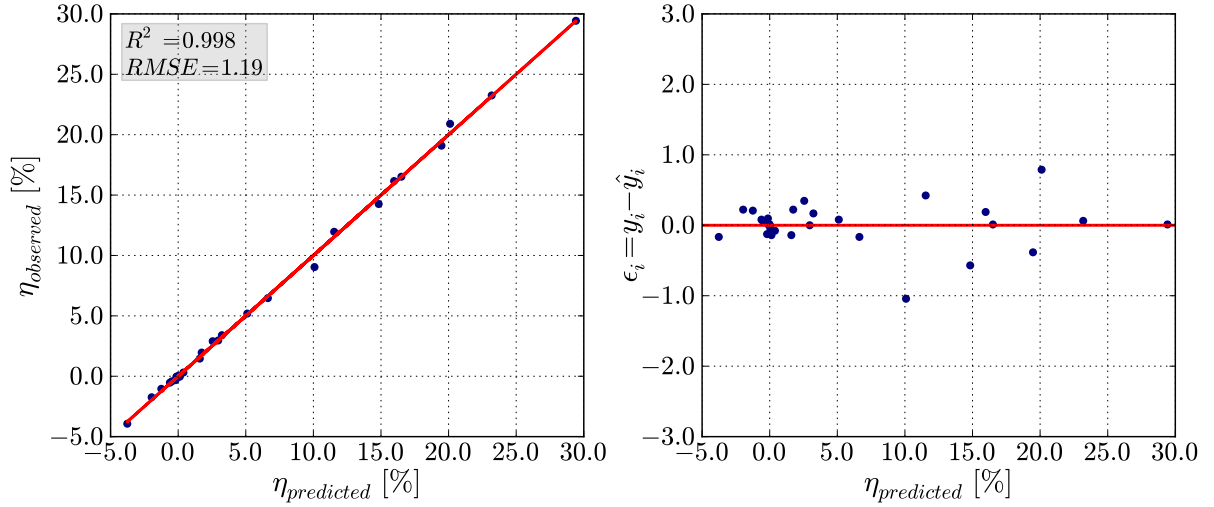


Figure 4: Predictions of surface response design. $R^2 = 0.998$.

The factors level that optimize the response are shown in the table (6). The maximum efficiency in the experimental domain is $\eta_{cycle} = 30.1\%$. The result on the coded variables reveals that the real optimum of this system is outside the experimental domain. Indeed, except for $\alpha_{out,stator}$, the optimal value of the factors is located on the boundary of the experimental domain. This is promising since it means that it is possible with this system to extract more than 30% of the injected energy into the turbine over a valve cycle, if the experimental domain is redefined.

	Π_1 h_{stator}/x_c	Π_2 h_{rotor}/x_c	Π_3 $\alpha_{out,stator}$	Π_7 $P_{t,open}/P_{s,outlet}$	Π_8 U_{rotor}/V_θ	Π_{10} $\Delta t_{open}/\Delta t_{cycle}$
Coded	+1	+1	+0.75	+1	-1	-1
Real	0.8	0.8	75°	3.0	0.25	0.1

Table 6: Factors optimizing turbine efficiency in the experimental domain ($\eta_{cycle,max} = 30.1\%$).

The position of the optimum gives the main trends for the design of a turbine fed by a pulsed flow, as far as 2D analysis can be applied. It reinforces the usefulness of the stator for this system. This result was not an evidence since the instantaneous performance is dictated by the waves propagation, and not by the usual steady analysis expressed by Euler's theorem. The stator must be composed of blades with a high solidity (h_{stator}/x_c) which forces a large deviation ($\alpha_{out,stator}$) to the flow. This kind of stator generates much more intense wave reflections and diffraction than if h_{stator}/x_c and $\alpha_{out,stator}$ were kept at their lowest levels. The reflections amplification causes an inlet energy flux reduction during the opening phases. The diffraction intensification, especially at the trailing edge, causes a large reduction in the transmitted waves intensity to the rotor. The rotor is then less sensitive to the flow unsteadiness. This behavior can be seen by comparing the standard deviation of the work signal between simulations $n^\circ 7$ and $n^\circ 27$, where only stator geometrical parameters are modified.

The rotor solidity h_{rotor}/x_c must also be high, table (6). The sensitivity estimation of the response surface shows that this factor is the most important for the turbine design. Observations of the DOE results, table (5), prove that it is impossible to reach high efficiency when h_{rotor}/x_c

is low. It is possible that this is due to the large recirculation zones that take place at the leading edge on the suction side of the rotor blades, and that persist more or less over time, when the stator geometrical factors are at their highest levels. Indeed, when the size of these zones is of the order of magnitude of the pitch, pressure profiles on both sides of the rotor blade tend to be the same. Therefore, h_{rotor}/x_c must be high enough to overcome this difficulty.

The table (6) reveals that the turbine is more efficient to extract energy when high pressure ratios are applied over a short ratio cycle. As well as the stator design, low ratios cycle attenuate the energy injected into the turbine over a cycle, while high pressure ratios increase it. This may seem contradictory. In addition, the unsteadiness related to the shock wave propagation during the valve opening is maximal for these cycle features. Indeed, for low cycle ratios, the upstream flow of the shock wave is mostly at rest in the stator. The downstream shock state is set by the inlet boundary condition, the shock wave intensity is then maximal for this cycle features³. As explained, stator reduces the unsteadiness that propagates to the rotor. A compromise must therefore be found between h_{stator}/x_c , $\alpha_{out,stator}$, $P_{t,open}/P_{s,outlet}$ and $\Delta t_{open}/\Delta t_{cycle}$ in order to reduce the energy flux through the turbine while maximizing the unsteadiness benefits within the rotor.

Finally, in order to minimize the drawbacks related to unsteadiness, more specifically compressor operation during the valve closing phase, Π_8 must be as low as possible. The smaller Π_8 , the lower the rotor speed compared to the characteristic bulk velocity.

CONCLUSIONS

Preliminary 2D design recommendations for a turbine driven by a pulsed flow have been given in this paper. In order to catch the main trends for the turbine design, a parametric study has been carried out. Recommendations were given on geometric and dynamic parameters which maximize a recovery ratio based on the amount of energy entering the control volume defined by the stage. 10 dimensionless parameters were selected as input of the degree of experiment. Response surface modeling was carried out on the influential factors following the screening design. The response surface calculation allowed to show the turbine characteristics maximizing η_{cycle} , see figure (5). The set of factors ($\alpha_{out,stator}$, h_{stator}/x_c , $P_{t,open}/P_{s,outlet}$, $\Delta t_{open}/\Delta t_{cycle}$) must allow to find a balance between minimizing the energy injected into the turbine and amplifying the benefits linked to the unsteadiness caused by the shock wave propagation during the valve opening. In addition, the rotor solidity (h_{rotor}/x_c) needs to be high so that the pressure distribution on both sides of the blade is not only controlled by the recirculation zones. Finally, the rotor speed must be low compared to the average bulk velocity in order to avoid the occurrence of compressor mode.

Now that a better knowledge of the factor influence and range is identified, a gradual increase in geometrical complexity is scheduled, in order to integrate 3D effects, and thickness distribution.

ACKNOWLEDGEMENTS

The authors would like to thank the DGA for their financial support and for permitting the publication of the research. This work was performed using HPC resources from GENCI-IDRIS (Grant 2020-100431), GENCI-CINES (Grant 2020-A0082A07178) and CALMIP (Grant 2020-p1425).

³This explains the compressor phases on the simulation $n^\circ 25$.

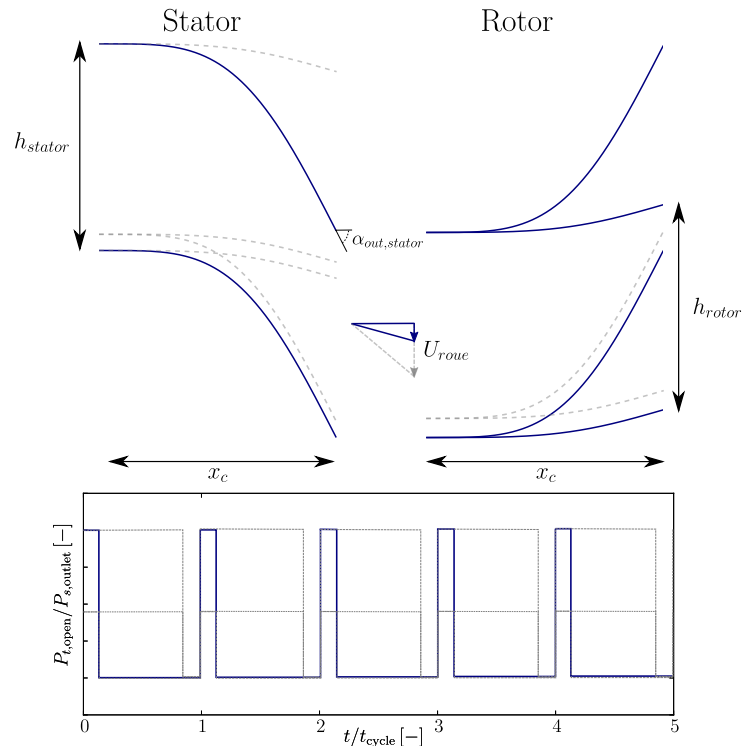


Figure 5: Design recommendation for a turbine driven by a pulsed flow. Recommendations are identified by lines (—). The lines (---) show the experimental domain. It should be noted that the speed triangle shown is a pictorial, albeit very inadequate, way of characterizing the rotor speed in relation to a semblance of flow speed.

References

- Baines, N. C. (2010), Turbocharger turbine pulse flow performance and modelling, 25 years on, Engineering Conferences Online.
- Brès, G. A., Ham, F. E., Nichols, J. W. & Lele, S. K. (2017), ‘Unstructured large-eddy simulations of supersonic jets’, *AIAA Journal* .
- Goupy, J. (2001), *Introduction aux plans d’expériences*, Technique et ingénierie Série Conception, 2e édition edn, Dunod, Paris.
- Hermet, F., Binder, N. & Gressier, J. (2019), Transient flow in infinitely thin airfoil cascade, in ‘Proceedings of 13th European Conference on Turbomachinery Fluid dynamics & Thermodynamics ETC13’, Lausanne, CH.
- Lee, J., Tan, C. S., Sirakov, B. T., Im, H.-S., Babak, M., Tisserant, D. & Wilkins, C. (2017), ‘Performance metric for turbine stage under unsteady pulsating flow environment’, *Journal of Engineering for Gas Turbines and Power* **139**(7), 072606.
- Liu, Z. & Copeland, C. (2020), ‘Optimization of a radial turbine for pulsating flows’, *Journal of Engineering for Gas Turbines and Power* **142**(5).
- JMP[©] (1989-2019), ‘Version 15.0. SAS Institute Inc., Cary, NC’. <https://www.jmp.com>.